JJMIE

Volume 16, Number 1, January. 2022
ISSN 1995-6665
Pages 123 - 131

Jordan Journal of Mechanical and Industrial Engineering

Mechanical Parts Pose Detection System Based on ORB Key Frame Matching Algorithm

Chun Liang*

School of Intelligent Manufacturing, Jiangsu Vocational Institute of Architectural Technology, Xuzhou 221000, China

Received 14 July 2021 *Accepted 28 December 2021*

Abstract

In order to solve the practical problem of accurate measurement of the position and posture of mechanical parts in the process of handling, a detection system for the position and posture of mechanical parts is designed. The improved Canny edge detection algorithm is used to recognize the contour of the mechanical part edge, and the scale invariant feature transformation method is used to extract the feature points and stereo matching of the mechanical parts. The mathematical model of the pose detection system is established, and the position and direction of the mechanical parts placed on the conveyor belt are calculated by solving the transformation relationship between coordinate systems. The shape and position of mechanical parts are recognized by compiling the pose recognition program. The experimental platform of pose test system is built and the test experiment is carried out. The experimental results show that the designed system can detect the position and orientation of parts quickly and effectively, and provide technical support for the realization of automatic pose detection of parts.

Keywords: ORB keyframe matching algorithm; Mechanical parts; Pose detection system; Canny edge detection.

1. Introduction

In the flexible automatic production line, robot is needed to carry, transfer and transport the mechanical parts. To grab a part, the robot first needs to measure the pose of the part [1]. It is the key technology of automatic feeding and unloading of parts to determine the placement, position and posture of the parts by the vision system. Machine vision is a kind of measuring and judging technology using machine instead of human eyes. In recent years, machine vision technology combined with robot technology has been widely used in industrial testing [2].

As a new non-contact technology, mechanical parts pose measurement technology can effectively make up for the shortcomings of the traditional 3D measurement, many experts at home and abroad have been widely concerned. The technology of measuring position and pose of mechanical parts has the advantages of real-time and high precision, which not only accords with the detection and positioning of intelligent factories, but also improves the automation and efficiency of industrial products [3]. The biggest advantage of non-contact position and pose detection is that the parts can be on-line detected and the following adaptive finishing can be carried out without reinstalling the parts. In the position and pose detection system of mechanical parts, the number of imaging pictures obtained by camera mainly includes many, binocular and monocular vision systems. Although the structure of monocular vision system is simple, it is difficult to measure the coordinate of depth in 3D coordinate. Binocular stereo vision is the use of two cameras in different positions to capture the same scene as a single camera after changes in position and pose [4]. Therefore, the study of binocular stereo positioning and pose detection is very meaningful, which can quickly and non-contact get the 3D coordinate information of parts, and calculate the pose.

In recent years, linear friction welding is an important method for machining and servicing aero-engine blades, and it can achieve better weld performance and integrated effect [5]. Because of the complex structure of the whole blisk, the machining technology is faced with great technical problems. Engine impeller is a kind of high precision machining product, and its machining quality affects engine performance. Therefore, the current disc processing technology has stopped the decentralized processing method, but adopted the overall processing method. At present, the way of machining integral blisk is concretely divided into welding and integral machining [6]. However, the overall processing of large quantities of materials and processing cycle is long, so linear friction welding is a good overall disk manufacturing means [7]. But after welding, the error detection of the position and attitude between blade and disk center is the key. After frictional linear welding, according to the position and posture obtained. At present, the visual inspection system is mainly used to detect the position of workpiece, but the research on the method of workpiece attitude inspection is less. Aiming at the actual demand of measuring the position and posture of mechanical parts in the process of transportation. This paper designs a position and posture detection system based on ORB (oriented fast and rotated brief) key frame matching algorithm.

* Corresponding author e-mail:liangchun1980@163.com

2. Conversion Scheme of Part Pose Detection System

2.1. Transformation of coordinate system of space coordinates

The system consists of 4 modules: image acquisition, image analysis and processing, dimension measurement and result output. The basic flow of the system is shown in Figure 1.

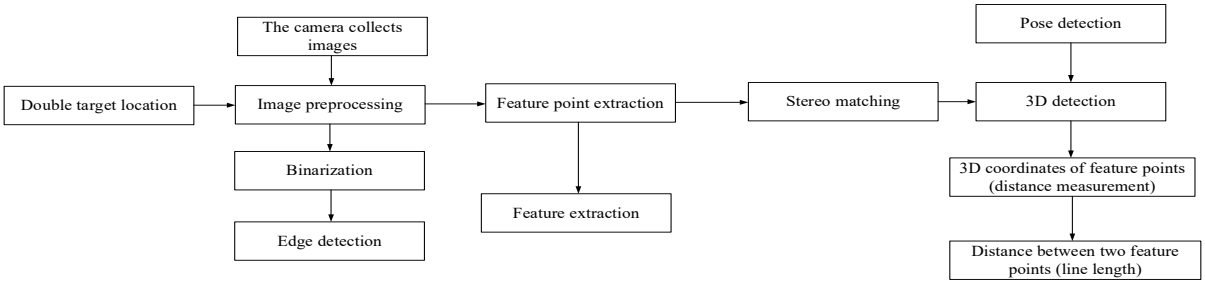

Figure 1. Work flow chart of pose detection system

In Figure 1, the position and attitude detection system is calibrated by using the calibration board, and then the image captured by the camera is binarized and edge detected, and the feature points are extracted from the image. Based on this, the points with the same features in the image are matched and the same name points are generated. Finally, the coordinates of the feature points, the external dimensions of the parts and the position and attitude information of the parts are measured through the 3D measurement module. The values of the coordinate system are represented by the position and orientation of the pixels. The origin is located at the top left corner of the pixel graph, the origin is located at the bottom of the V axis, and u axis is to the right, respectively representing the column pixels and row pixels. The coordinate conversion diagram of the spatial coordinate system is shown in Figure 2.

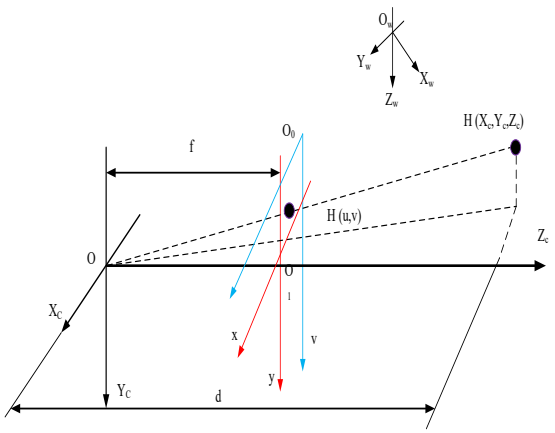

Figure 2. Transformation diagram of space coordinate system

2.2. Image gray level transformation

Mechanical part recognition needs to scan the part image by the camera first, and then transmit the acquired image to the PC through the image acquisition card. In the whole process of image collection, the quality of the collected image will be affected by various factors. Therefore, before the detection of mechanical parts, it is necessary to process the digital signal. In this way, the image distortion can be avoided as much as possible [8]. Therefore, it is very important to develop image preprocessing.

The general display consists of a finite number of points, and the points in this series are called pixels. The coloring device colors each pixel from left to right, and then colors all the pixels in the screen from top to bottom; people can feel the image information through the short visual effect of the eyes. Bitmaps display and save images through bitmaps [9]. Bitmaps include color bitmaps and grayscale images. Color bitmaps are formed by mixing red, green, and blue (R, G, B) colors, with different proportions of each color forming a variety of new colors. However, all pixels of all images are described by RGB components, which will eventually lead to the result that most of the computer storage space will be occupied by images. Grayscale image is a kind of non-color-table image described by different illumination intensity. It can express the grayscale image by quantifying the brightness value. Gray-scale map is generally divided into 0-255, where 0 represents pure black, 255 represents pure white.

Grayscale is one of the common ways of digital image information processing. There is an equal transformation relationship between image RGB color and gray value. In the RGB color mode of the image, a set of (RGB) values are used to represent the color information, which can be converted with the gray level of the image. After grayscale processing, the color and brightness of color image can be converted to the brightness of grayscale image. For RGB, the values are set to be equal, so the RGB value is changed from (0, 0, 0) to (255, 255, 255), (0, 0, 0) to pure black, (255, 255, 255) to pure white, and (0, 0, 0) to (255, 255, 255) to gray. In this way, we can use RGB value to describe the gray image.

Through image gray-processing, it can greatly reduce the workload of PC, shorten the image processing time, can get more detailed image information, greatly reduce the interference of external factors, and reduce the image processing difficulty [10]. Therefore, it is most reasonable to use gray-scale image in machine vision recognition and inspection.

There are three methods for gray scale transformation: maximum method, average method and weighted average method.

Maximum value method: the component with the largest value among RGB components is regarded as the gray value of the pixel. The formula is as follows:

$$R = G = B = \max(R, G, B) \tag{1}$$

The brightness of the image obtained by this method is high.

Average Value Method: Take the average of the three RGB components as the gray value of this pixel. The formula is as follows:

$$R = G = B = \frac{\max(R, G, B)}{3} \tag{2}$$

The images obtained by this method are more harmonious.

Weighted average method: to make certain proportional values of the three components of RGB according to certain rules, calculate the weighted average values of the three components and treat the values as gray values. The formula is as follows:

$$R = G = B = \frac{(W_R R + W_G G + W_B B)}{3} \tag{3}$$

where W_R, W_G and W_B are the weight values of RGB components. By changing the values of W_R, W_G and W_B, various gray images can be produced. It is found that people have the strongest light sensitivity to the green series, but the least sensitive to the blue series. In this study, weighted average method is used.

For the light between the green and blue series, according to the $W_R > W_G > W_B$ weight value, we can get the gray image which is more suitable for human eyes. In particular, in W_R=0.299, W_G=0.587, W_B=0.114 values, the human eye is more likely to feel the color of the light.

3. Image Preprocessing of Mechanical Parts Position and Pose Detection System

Due to the influence of external environment and internal parameters, such as illumination, lens, etc., in the process of image acquisition, the image of mechanical parts will be disturbed. If the angle of illumination causes the surface of the workpiece to be obscured by light from the environment, or to reflect light resulting in highlighting, or the workpiece is located on a platform showing signs of irregularity [11, 12]. Because the camera has a strong ability to capture images, these external effects will be captured by the camera and presented in the image, which is easy to cause image misjudgment, so image preprocessing is needed. There are three main steps in image preprocessing: image binarization, edge contour extraction, and mass processing (connected domain).

3.1. Image binarization

Because the principle of black-and-white image data is simple and reliable, it can be easily identified by computer. The binary method is used to process the image, and all the gray information of the image is converted into 0 and 255 binary values. Position and pose detection systems for mechanical parts minimize interference from object color properties [13]. In this paper, Otsu method is used to binarize the image. The idea of Otsu algorithm is to divide the image into background and target, and the larger the variance between the background and target, the greater the difference between the two parts. Therefore, maximizing the variance between classes means minimizing the probability of misdivision.

For the image gray value $K(x, y)$, the segmentation threshold of target and background is marked as H, then there are:

$$\begin{cases} w_0 = \dfrac{N_0}{M} \times N \\ w_1 = \dfrac{N_1}{M} \times N \\ N_0 + N_1 = M \times N \\ w_0 + w_1 = 1 \\ u = w_0 u_0 + w_1 u_1 \\ g = w_0 (u_0 - u_0)^2 + w_1 (u_1 - u_1)^2 \end{cases} \tag{4}$$

where: w_0 represents the proportion of target pixel points in the whole image; u_0 represents the average gray level; w_1 represents the proportion of background pixel points in the whole image; u_1 is the average gray level; u is the total average gray level of the image; g is the inter class variance; $M \times N$ is the size of the image when the background is dark; N_0 is the number of pixels whose gray value is less than the threshold T; N_1 is the number of pixels whose gray value is greater than the threshold T.

By simplifying Formula (4), the following can be obtained:

$$g = w_0 w_1 (u_0 - u_1)^2 \tag{5}$$

By using traversal method, the threshold T is obtained when the variance between classes is maximized. The optimal threshold value obtained by Otsu algorithm is 177. The ORB framework proposed in this study is an improved method based on graph optimization, and its overall framework is shown in Figure 3.

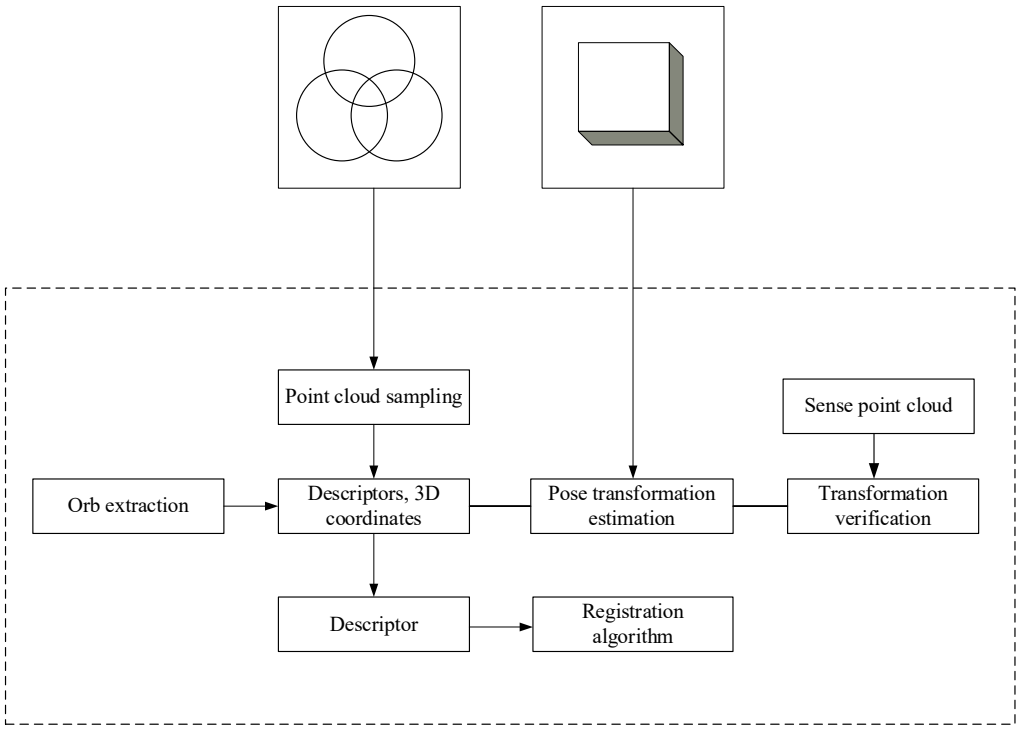

Figure 3. Improved ORB system framework diagram

The framework is divided into three parts: front-end construction, back-end optimization and map representation. According to the observation and constraint information, the system can construct the position and pose map and the 3D point cloud by feature point registration and position and pose transformation.

3.2. Extraction of part edge contour

Part edge reflects the structural characteristics of the part, so before the image recognition, image edge detection, effectively reduce the computer misjudgment of the measured parts [14].

In this paper, the improved Canny edge detection algorithm is used to detect the edge of parts, and the gradient amplitude calculation method is used to improve it.

The basic process is as follows: denoising the image by Gauss; interpolating all the pixels in the neighborhood along the gradient direction with the gradient amplitude, calculating the gradient direction and amplitude, detecting the maximum amplitude points, and then getting the edge points; then suppressing the non-maximum value, then connecting the edges through the double threshold algorithm to prevent false edges from appearing in the contour map, and improving the efficiency of part edge calculation [15].

3.3. Image block processing

Image agglomeration processing is to process the connected region of the image. The measurement system of the position and orientation of the parts remove the connected region that is smaller than the region value by setting the value of the area and the perimeter domain, and by successively removing the connected region through the processes of removing the noise of the perimeter, the area and the roundness domain [16, 17].

For example, in binarization image, the uneven part of the workpiece surface is displayed on binarization image because of the influence of the illumination angle.

***3.4.** Image preprocessing experiment*

After calibration by the calibration board, the system places the workpiece to be measured (in the middle of the camera picture). In this study, "Otsu binarization" method is used to preprocess the part image [18].

The Canny edge detection algorithm is used to detect the edge of parts. In this process, Gaussian filter is needed to filter out the interference information. In the Gaussian filter, the Gaussian kernel can be regarded as the weight negatively correlated with the center distance. During image smoothing, adjusting the standard deviation σ of Gaussian filter is actually adjusting the influence of surrounding pixels on the current pixel. Increasing σ increases the influence of distant pixels on the central pixel, and the smoother the image filtering result. The calculation process of spatial standard deviation σ of Gaussian filter is as follows:

$$\sigma=\frac{1}{2\pi\sigma_{\omega}} \tag{6}$$

where σ_{ω} represents the standard deviation corresponding to Gaussian in frequency domain. In this study, the standard deviation σ of Gaussian filter is set to 0.4, and the edge detection effect is shown in Figure 4.

(a) Left camera capture screen (b) Right camera capture screen

Figure 4. Edge detection image

4. Stereo Matching and Part Pose Detection

4.1. ORB feature point detection and matching

The ORB algorithm extracts feature points through FAST corner detection. Its principle description is as follows: for detecting the gray value of 16 pixels in a circle with any point p as the center and 3.4 pixels as the radius (referred to as the M16 template), if the gray value of consecutive n points in M16 is greater than Ip t or less than $I_p - t$ (among which: $I_p - p$ point gray value, t −threshold), p shall be determined as the feature point. In order to improve the speed and accuracy of feature point detection, the author adopts a segmentation test standard, namely 12 point detection method. Only the gray values of points 1, 5, 9 and 13 are detected first, and the remaining 12 points are detected only after at least 3 points meet the above threshold conditions [19]. The M16 test template is shown in Figure 5.

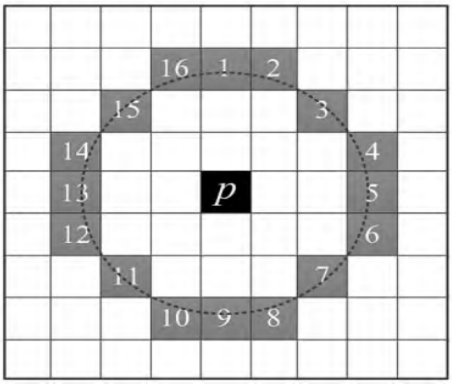

Figure 5. M16 test template

The above segmentation criteria only apply to the case of n = 12. In order to improve the accuracy and effectiveness of detection, the machine learning method is introduced into the FAST algorithm. The steps are as follows: for the specified pixel value n and threshold t, all feature points are detected from the image set by using the segmentation test criteria. The process needs to detect the M16 of each point, and the detected image is used as the training sample [20]. Then, according to the principle of maximum information gain, the ID3 algorithm is used to train the feature point classification decision tree. The points in the image are classified into feature points and non-feature points by decision tree.

The system backend is responsible for the optimization of the posture map, so that the output map model has global consistency. Sensor noise, cumulative error of depth value quantification and registration error will lead to the uncertainty of the system, and then pose and drift of 3D map will appear [21]. Through closed-loop detection, random closed-loop detection and trajectory optimization, the whole map is updated in real time in order to enhance the global consistency of the generated map model.

The fast corner detection based on machine learning only compares the pixel gray values, so that its matching efficiency is effectively improved. Machine learning can enhance the universality of the algorithm. If the intensity centroid is specified as the rotation direction, the rotation invariant of fast (oriented fast) descriptor can be obtained [22]. The process is as follows: take the feature point O as the origin of the coordinate system, calculate the centroid position B in the neighborhood P, and construct the vector $\overrightarrow{OB}$ with the feature point as the starting point and the centroid as the end point.

The matrix of a neighborhood can be expressed as:

$$R_{as} = \sum_{n \times m} x^a y^s K(x, y) \tag{7}$$

where: $K(x, y)$ is the gray value of the image, $x, y \in [-r, r]$, and r is the radius of the neighborhood P. Then the centroid position of the neighborhood is:

$$C_u = \left(\frac{R_{10}}{R_{00}}, \frac{R_{01}}{R_{00}} \right) \tag{8}$$

In order to detect the pose of workpiece in binocular stereo vision system, it is necessary to detect and match feature points. Stereo matching is to find the conjugate image points in the collected left and right images, and determine the corresponding relationship between the target points in the left and right images. Pose is the position and posture of the object, where the position is the coordinate value of X, Y and Z, and the posture is the rotation angle around X, Y and Z. Make the point set $P_{1i} = (x_{1i}, y_{1i}, z_{1i})$ at the ideal position before welding and $P_{2i} = (x_{2i}, y_{2i}, z_{2i})$ after welding. Therefore, the coordinate value of P point before welding is formed by a rotation matrix and a translation matrix, which is as follows:

$$\begin{bmatrix} x_{2i} \\ y_{2i} \\ z_{2i} \end{bmatrix} = R \begin{bmatrix} x_{1i} \\ y_{1i} \\ z_{1i} \end{bmatrix} + T \tag{9}$$

where vector T is a three-dimensional vector:

$$T = [tx, ty, tz]^T \tag{10}$$

The translation vector T is the position translation of two pieces before and after welding, and the R matrix is a 3×3 matrix, in which nine elements are trigonometric functions of three angles (R_x, R_y, R_z), and R_x, R_y and R_z are the three rotation angles around axis X, Y and Z of boss coordinate system respectively. The detailed rotation process is as follows: first, Z rotates around axis R_z, then rotates R_y around axis Y, and finally rotates R_x around axis X. the right hand rule is positive.

4.2. Extraction and stereo matching of feature points

The system utilizes the scale invariant feature transform (SIFT) based on feature point scale invariant feature transform for stereo matching. SIFT is a widely used feature point detection and description algorithm at present. The key of SIFT feature matching is to extract feature points. The extraction process of feature points is as follows: detecting the extreme value of scale space, determining the correct feature points and the main direction of feature points, and generating SIFT feature vectors. The specific steps are as follows:

(1) Computing the point-to-point test based on child windows in the neighborhood of a certain feature point;

(2) Sort all the test values in step (1) according to the difference between them and 0.5 to form a vector;

(3) Greedy search: (a) placing the first test point in the result vector R and removing it from the vector; (b) taking a test from the vector and comparing it with all the test values in the vector, and discarding it if the correlation is greater than a certain threshold, or adding it to the vector as a coordinate to generate the descriptor; and (c) repeating the above steps until there are 256 coordinates in the vector to form the final descriptor. Then the correlation threshold is increased, and the correlation of the selected test values is checked again to ensure that the final results have a smaller correlation.

The detection of the change of position and orientation of welding parts. Firstly, the technology structure of finishing square convex table on the blade blank is shown in Figure 6, which is used for blade positioning.

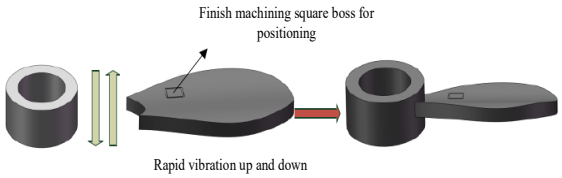

Figure 6. Sketch of linear friction welding of bladed disk

Before welding, fix the vane disc in the ideal position of the disc center with special fixture. Firstly, a mark circle is pasted on the convex platform, a vertex is selected, and three vertical boundaries are made as the coordinate system of X, Y and Z axis. After the welding, the images of the boss are taken and the 3D coordinates are calculated. Finally, we get the 3D coordinates and calculate the angle of the three translation parameters R_x, R_y and R_z in the convex coordinate system.

The position and posture detection system detects the coordinates of X, Y and Z of some key points by binocular stereo vision, and solves the displacements of three coordinate axes and the corners of three states according to the coordinates. Finally, the tool path is generated by NC programming and the blank parts are finished. The gray transparent portion is the extra margin in Figure 7.

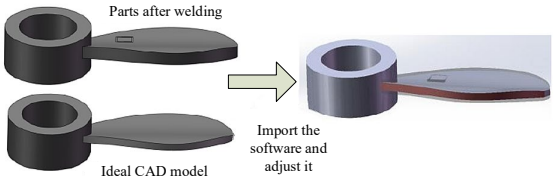

Figure 7. Comparison of parts and ideal part models after determination of welding pose

4.3. Modeling of pose detection system

In essence, the pose detection of parts is to solve the position relationship between two coordinate systems. There are two groups of parameters to describe the pose transformation of two coordinate systems: Euler angle and displacement. Firstly, a workpiece coordinate system is established on the part to be measured. The origin can be set at the space position on or near the part. The coordinate system is marked as OM and the world coordinate system is marked as Ow. The OM coordinate system is rotated around ZM axis. When XM axis (YM axis) is parallel to ow's XW axis (Yw axis), the rotation stops and the rotation angle γ is recorded. Suppose that the parallel axes are XM and Xw, then rotate the OM coordinate system around the XM axis until the second coordinate axis is parallel; assume that the second parallel axis is YM and Yw, record the rotation angle β; the last rotation makes OM parallel to Ow three axes, and then record the rotation angle α.

The coordinate system OM translates along the three directions of X, Y and Z, and finally completely coincides with Ow. The displacement of the translation is the three-dimensional coordinates XT, YT, ZT of the origin of the OM coordinate system in Ow. In fact, the pose of a part is the transformation of two coordinate systems.

The steps for measuring the pose of the part are as follows:

(1) Establishing the relationship between the reference coordinate system and the camera coordinate system. The space vectors of each axis of the coordinate system are obtained by using the method of plane fitting, and the space vectors of 3 axes in the camera coordinate system are constructed.

(2) Obtain the position relationship between the workpiece coordinate system and the camera coordinate system in real time. The coordinate values of the points in the coordinate system of the workpiece are obtained by identifying the feature points on the part, and the coordinate values of the points in the camera coordinate system are obtained by measuring the feature points.

(3) Obtain the position relationship between the workpiece coordinate system and the reference coordinate system. According to the relation obtained in step (2) and the relation between the reference coordinate system and the camera coordinate system, the position relation matrix of the two systems is obtained by matrix transformation.

(4) Solve the pitch angle, yaw angle and roll angle of the workpiece in the reference coordinate system.

The relationship between the workpiece coordinate system and the reference coordinate system determines the position of the partial angle of the part relative to the reference coordinate system, that is, the space attitude of the part. It is determined by three angles describing the relative relationship between the two coordinate systems, namely, the Euler angle, as shown in Figure 8.

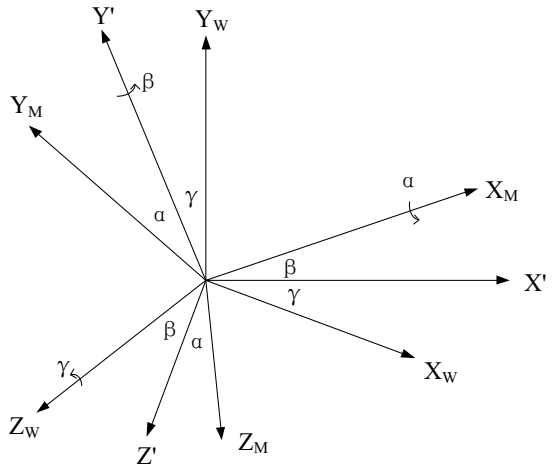

Figure 8. Relationship between reference coordinate system and moving body coordinate system

In Figure 8, the pitch angle alpha represents the angle of rotation of OYM 'around OXM to OYM, that is, the angle between OYM and the plane OXM Y'. The angle of yaw beta represents the angle of rotation of OX 'around OY' to OXM, that is, the angle between OXM and plane OZW X'. Roll angle γ represents the angle of rotation of the OXW axis around the OZW axis to the OXW axis in the reference coordinate system, that is, the angle between the OXW axis and the plane OXW ZW. The angle sign is determined by the right-hand rule.

5. Testing Experiment and Error Analysis of Parts Position and Pose

5.1. Parts and posture testing platform

In the simulation, the hardware environment: Celeron 2.4 GHz for the processor, 4GB of memory for the computer, Windows 7 for the software environment, using C + in the Visual Studio compiler. Testing experimental time was 30 min.

In order to verify the effect of part pose detection, a platform for part pose detection is built, as shown in Figure 9.

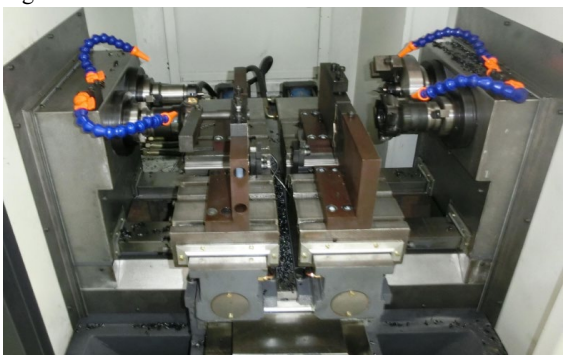

Figure 9. Binocular stereo vision measurement system platform

As can be seen from Figure 9, there are two parts of the instrument. Other specific platforms include: binocular calibration, binocular detection, stereo matching, binocular measurement, pose and angle measurement.

5.2. Part pose testing process

After actual measurement and parameter adjustment, the distance between each point of the calibration board and the left camera (the origin of the coordinate system coincides with the light center of the left camera) is approximately equal to the Z-direction value of the three-dimensional coordinates of the workpiece under measurement. Taking the six-hole workpiece as an example, the posture measurement is carried out. Select 5 feature points of the workpiece to measure, use 3 feature points to establish a workpiece coordinate system, and use 2 feature points for accuracy correction. The position and posture of the six-hole workpiece are tested by placing the workpiece in any of six positions. The specific flow is shown in Figure 10.

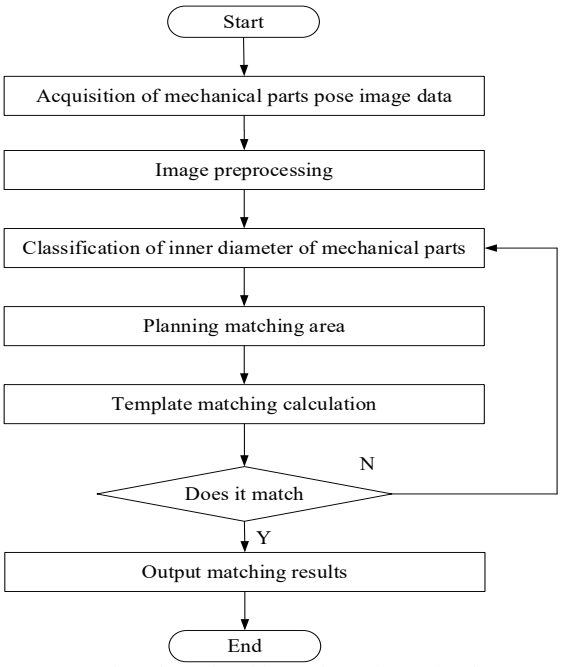

Figure 10. Flow chart of position and pose inspection for mechanical parts

5.3. Experimental error

The experiment is divided into two groups, the first group of tilted, the second group of vertical and horizontal direction of placement, left and right side of the detection of the screen as shown in Figure 11.

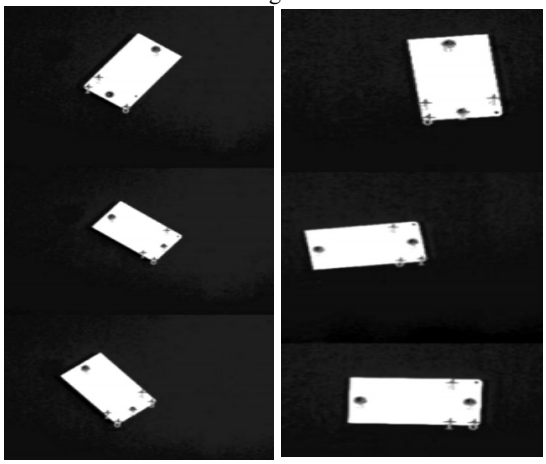

(a) Left instrument test drawing (b) Right instrument test drawing

Figure 11. Six hole workpiece placement posture

Measure the 6 positions of the parts, and get 6 sets of pose data, as shown in Table 1.

Table 1. Position and orientation data table of six holes

Position	Pitch angle (°)	Yaw angle (°)	Roll angle (°)
1	19.83	176.89	-106.25
2	36.44	-15.45	-155.45
3	84.82	-77.65	-99.45
4	84.26	54.26	170.69
5	52.36	8.89	115.28
6	58.14	-30.25	-127.65

In order to verify the accuracy of the position and pose measurement system, the position and pose of workpiece

No. 5 is repeated for 5 times. The results are shown in Table 2.

Table 2. Test data of position and pose of workpiece No. 5

Position	Pitch angle (°)	Yaw angle (°)	Roll angle (°)
1	53.25	8.95	115.25
2	53.26	8.54	115.89
3	53.12	9.01	114.15
4	53.30	9.52	114.69
5	53.45	8.90	117.86

In Table 2, the measurement of the angle of rotation of the workpiece around the X and Y axes has a slight fluctuation, with only a deviation of 0-0.54°and 0-1.03°; The measurement of the angle of rotation along the Z axis has a larger deviation, with a maximum of 3.42°. Generally, the parts are transported by adsorption, which requires high precision in X and Y direction and is insensitive to Z-axis deviation. Therefore, the system can meet the requirements of parts loading and blanking.

Using the same computer, we compare several common feature points extraction and matching algorithms by artificial rotation and Gaussian noise. The matching results can verify the rotative invariance of the improved ORB algorithm. As shown in Figure 12, the improved ORB algorithm proposed in this study has better anti-rotation performance than other algorithms.

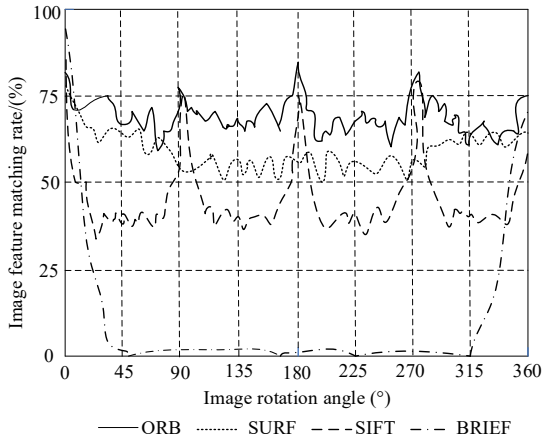

Figure 12 Comparison of various algorithms for rotation invariance

As can be seen from Figure 12, the execution time of the algorithm is an important indicator of the real-time performance of the algorithm. Under the same hardware conditions, using the atlas of data set can verify that the ORB operator has better real-time performance. The matching feature points are extracted by ORB algorithm, and the feature point descriptor D-R64 is stored in the form of Y-R3. The geometric relationship between the observed position (X-R6) and the observed information can be obtained. Through the inter-frame registration of ORB feature point image, the feature data in different observation coordinate system can be transformed into global coordinate system to detect the position and orientation of mechanical parts.

Finally, taking the pose detection accuracy as the index, the application performance of different methods is verified, and the results are shown in Table 3.

Table 3 Comparison results of pose detection accuracy of different methods (%)

Image rotation angle (°)	ORB	SURF	SIFT	BRIEF
90	93.26	87.89	75.24	82.36
180	94.27	88.55	75.88	83.41
270	94.13	89.02	74.14	83.60
360	95.31	89.50	74.64	84.14

By analyzing the results shown in Table 3, we can see that with the change of image rotation angle, the pose detection accuracy of different methods also changes. However, in contrast, the pose detection accuracy of this method can always be maintained at more than 90%, which is significantly higher than the three traditional methods, which proves that this method has better application effect.

6. Conclusions

Based on the ORB key frame matching algorithm, the position and pose detection system of mechanical parts is designed. According to the actual requirements of position and pose detection in the process of loading and unloading of mechanical parts, this paper designs a set of pose detection system for mechanical parts, establishes the mathematical model of pose detection system by using ORB key frame matching algorithm, and calculates the parts in the conveyor belt by solving the transformation relationship between coordinate systems The algorithm program of pose recognition is compiled to realize the recognition of the shape and pose of parts. The test experiment is carried out with a typical workpiece as an example. The experimental results show that the system can quickly locate and measure the parts and meet the requirements of loading and unloading of mechanical parts.

Acknowledgement

The research is supported by: Ministry of housing and urban rural development science and technology program (No. 2016-K4-063).

References

[1] Leicht A, Yu C H, Luzin V, et al. Effect of scan rotation on the microstructure development and mechanical properties of 316L parts produced by laser powder bed fusion. Materials Characterization, 2020, 163(5): 110-118.

[2] Vicente C M S, Martins T S, Leite M, et al. Influence of fused deposition modeling parameters on the mechanical properties of ABS parts. Polymers for Advanced Technologies, 2020, 31(3): 501-507.

[3] Sánchez-Safont E L, Arrillaga A, Anakabe J, et al. PHBV/TPU/cellulose compounds for compostable injection molded parts with improved thermal and mechanical performance. Journal of Applied Polymer Science, 2018, 28(5): 1-13.

[4] Azarniya A, Colera X G, Mirzaali M J, et al. Additive manufacturing of Ti–6Al–4V parts through laser metal deposition (LMD): Process, microstructure, and mechanical properties. Journal of Alloys and Compounds, 2019, 804(2): 15-26.

[5] Johnson L E. Chokepoints in mechanical coupling associated with allosteric proteins: the pyruvate kinase example. Biophysical Journal, 2019, 116(9): 1598-1608.

[6] Ramírez-Muñoz J E, Restrepo C J P, Vinck-Posada H. Indirect strong coupling regime between a quantum dot and a nanocavity mediated by a mechanical resonator. Physics Letters A, 2018, 382(15): 3109-3114.

[7] El-Zayat M M, Mohamed M A, Shaltout N A. Effect of maleic anhydride content on physico-mechanical properties of γ-irradiated waste polypropylene/corn husk fibers bio-composites. Radiochimica Acta, 2020, 108(2): 151-157.

[8] Wesierski D, Jezierska A. Instrument detection and pose estimation with rigid part mixtures model in video-assisted surgeries. Medical Image Analysis, 2018, 46(30): 244-265.

[9] Tejani A, Kouskourida R, Doumanoglou A, et al. Latent-class hough forests for 6DoF object pose estimation. IEEE Transactions on Pattern Analysis and Machine Intelligence, 2018, 40(1): 119-132.

[10] Sharma S, Ventura J, D'Amico S. Robust model-based monocular pose initialization for noncooperative spacecraft rendezvous. Journal of Spacecraft and Rockets, 2018, 55(6): 1414-1429.

[11] Li J G. Distributed multi-level inventory algorithms for automotive maintenance spare parts based on centralized control model. Jordan Journal of Mechanical and Industrial Engineering, 2020, 14(1): 89-99.

[12] Berrington A, Voets N L, Larkin S J, et al. A comparison of 2-hydroxyglutarate detection at 3 and 7T with long-TE semi-LASER. Nmr in Biomedicine, 2018, 31(5897): 25-31.

[13] Mademlis I, Tefas A, Pitas I. A salient dictionary learning framework for activity video summarization via key-frame extraction. Information Sciences, 2018, 432: 319-331.

[14] Seke E, Anagün, Y, Adar N. A new multi-frame super-resolution algorithm using common vector approach. IET Image Processing, 2018, 12(12): 2292-2299.

[15] Ferrari R, Cocchetti G, Rizzi E. Effective iterative algorithm for the limit analysis of truss-frame structures by a kinematic approach. Computers & Structures, 2018, 197(1): 28-41.

[16] Xu Q S, Zheng H D, Hu Z, et al. High-precision parts image defect feature fast positioning retrieval simulation. Computer Simulation, 2019, 36(4): 413-417.

[17] Ning P F. An adaptive scheduling method for resources in used automobile parts recycling. Jordan Journal of Mechanical and Industrial Engineering, 2020, 14(1): 53-60.

[18] Sathya S P A, Srinivasan R. Non-redundant frame identification and keyframe selection in DWT-PCA domain for authentication of Video. IET Image Processing, 2019, 14(2): 26-32.

[19] Bommisetty R M, Prakash O, Khare A. Keyframe extraction using Pearson correlation coefficient and color moments. Multimedia Systems, 2020, 116(26): 1-33.

[20] Sathya S P A, Ramakrishnan S. Non-redundant frame identification and keyframe selection in DWT-PCA domain for authentication of video. IET Image Processing, 2020, 14(2): 366-375.

[21] Ferrari R, Cocchetti G, Rizzi E. Effective iterative algorithm for the limit analysis of truss-frame structures by a kinematic approach. Computers & Structures, 2018, 197(12): 28-41.

[22] Oyebode O A, Erukainure O L, Ibeji C, et al. Crassocephalum rubens, a leafy vegetable, suppresses oxidative pancreatic and hepatic injury and inhibits key enzymes linked to type 2 diabetes: An ex vivo and in silico study. Journal of Food Biochemistry, 2019, 43(8): 129-135.